XXXVI Ibero-Latin American
Congress on Computational
Methods in Engineering

CILAMCE

Rio de Janeiro, 22-25 Nov 2015

A MULTI-SCALE APPROACH TO MODEL ARTERIAL TISSUE

Felipe Figueredo Rocha

Pablo Javier Blanco

felipefr@lncc.br – pjblanco@lncc.br

LNCC/MCTI Laboratório Nacional de Computação Científica, INCT-MACC Instituto Nacional de Ciência e Tecnologia em Medicina Assistida por Computação Científica, Getúlio Vargas 333, Petrópolis, Rio de Janeiro, CEP: 25651-075, Brazil

Pablo Javier Sánchez

psanchez@intec.unl.edu.ar

CIMEC-UNL-CONICET, Colectora RN N° 168, Km 472, Paraje el Pozo, CP 3000, Santa Fe, Argentina

GIMNI-UTN-FRSF, Lavaise 610, CP 3000, Santa Fe, Argentina.

Alfredo Edmundo Huespe

ahuespe@intec.unl.edu.ar

CIMEC-UNL-CONICET, Colectora RN N° 168, Km 472, Paraje el Pozo, CP 3000, Santa Fe, Argentina

CIMNE, Centre Internacional de Metodes Numerics en Enyinyeria, Campus Nord UPC, Edifici C-1, J. Girona 1-3, 08034, Barcelona, Spain

Raúl Antonino Feijóo

feij@lncc.br

LNCC/MCTI Laboratório Nacional de Computação Científica, INCT-MACC Instituto Nacional de Ciência e Tecnologia em Medicina Assistida por Computação Científica. Getúlio Vargas 333, Petrópolis, Rio de Janeiro, CEP: 25651-075, Brazil

Abstract. *To gain insight on the onset and progress of some cardiovascular diseases, as well as to propose adequate treatments, a detailed characterization of the*

mechanical behaviour of the arterial wall is required. The classical constitutive modelling approach based purely on phenomenological laws fails in representing the micromechanical phenomena, which dominates important aspects such as rupture and remodelling of these tissues. In turn, the multi-scale constitutive modelling raises as a more rational alternative allowing to consider the microscopic details and interactions of the basic unit blocks of the biological tissues, such as the existence of the collagen fibres, pores, etc. In this paper, we review a constitutive multi-scale theory based on the existence of Representative Volume Element (RVE) in the finite strain regime, which is presented in a variational formulation framework. The homogenisation of the displacement and deformation gradient as well the virtual power equivalence between macro- and micro-scales through an extended version of the Hill-Mandel principle, are assumed as fundamental hypotheses of the model. As a result, we obtain the homogenisation of the macro-scale stress and the RVE equilibrium problem. The constitutive tangent operator is used to analyse the loss of stability of the macroscopic material response. This allows us to model macroscopic crack nucleation induced, for instance, by strain localization phenomena due to microscopic shear bands, damage or any other possible microscopic failure mechanism. In this context, preliminary results are discussed on the light of the present theoretical framework.
Keywords: *Multiscale Modeling, Representative Volume Element, Finite Strain, Variational Formulations, Failure*

1 INTRODUCTION

Cardiovascular diseases are being the leading cause of death worldwide Mendis (2011); Heidenreich et al. (2011). Accordingly, the efforts of the scientific community towards a more detailed understanding of this subject have increased during the last years. Due to complexity of the problem, the computational mechanics approach has become a viable and fundamental methodology to guide research on the field.

From a microscopic point of view, the arterial tissue is heterogeneous by nature. These heterogeneities (for instance, different families of fibres, voids, etc.) govern the mechanical response of the tissue at the macroscopic level. Thus, the RVE-based multi-scale variational approach arises as a powerful modelling tool to describe its constitutive behaviour Speirs et al. (2008).

The multiscale RVE-based formulation has been cast in a variational framework by de Souza Neto and Feijóo (2006, 2008), for both infinitesimal and finite strains. Such approach is adopted in this text, however with some important modifications. One of them is a generalization of the Hill-Mandel Principle of Macrohomogeneity, originally proposed in Hill (1965), which takes into account not only the internal virtual power but also the counterpart related to the external loads. This is important for modelling body forces varying at the microscopic level. Such extension is based on the general foundations for this kind of multiscale models recently developed in Blanco et al. (2014a,b).

A point of great practical relevance where the multi-scale modelling can give fruitful results is the study of degradation and failure of biological tissues. This approach allows us to study the nucleation of failure zones or cracks in the material at the microscopic level. The evolution and propagation of these micro-scale degradation mechanisms induce macro-scale failure modes, whose final representation is a macro-scale discontinuity or crack Sánchez et al. (2013). Failure in biological tissues is related to several diseases such as aneurysm growth and rupture and atherosclerotic plaque rupture, just to mention a couple of the more drastic and life-threatening cerebrovascular and cardiovascular events.

Another aspect that justifies the use of a multi-scale approach, is the difficulty to obtain parameters for tissue phenomenological models, since the experimental tests are normally performed *ex vivo* [1]. Thus, since one cannot improve the phenomenological models without requiring more material parameters, one solution is to make use of the mechanical interactions among the more basic building blocks of the tissues and to couple these micro-mechanisms with macro-models using a multi-scale strategy.

In addition the constitutive nonlinearities and the multi-scale nature of the biological tissues, there are still some others difficulties for modelling these materials. In one hand, biological tissues have to be modelled using a finite strain setting. Furthermore, unlike most engineering materials, there are some intricate evolving mechanisms such as growth and remodelling that change, among other aspects, the geometry and properties of the original tissues.

This work addresses the theoretical foundations and some mechanical considerations which are fundamental to address the multi-scale modeling of biological tissues in the precritical regime, that is, in the phase prior to macroscopic material instabilities arise. Phenomena includes degradation of micro-scale tissue components until the mechanical response of the RVE results in an unstable macro-scale classical model, for whose further analysis will ultimately require the mathematical and mechanical regularization through any suitable approach.

2 ARTERIAL WALL STRUCTURE

The human body is a highly complex system, in particular arterial wall tissue has a very rich composition from the mechanical point of view. The main structurally important components are elastin, collagen and smooth muscle fibres, as can be seen in Fig. 1(a). The basic description of each layer is the following:

***Intima*:** It consists mainly of elastin, which has almost a linear elastic and isotropic behaviour. Sometimes the endothelium is not considered part of this layer, due to the small thickness and low mechanical relevance.

***Media*:** It is the intermediate layer which comprises most of the artery. It is formed by an elastic and smooth muscle matrix reinforced with collagen fibres. Due to its structure, the mechanical behaviour of this layer is nonlinear and anisotropic.

***Adventia*:** It is the stiffest layer due to the high concentration of collagen fibres immersed in elastin.

As mentioned earlier, the media and adventia have anisotropic mechanical responses, for which the preferred collagen fiber orientation angle is a fundamental data. These angles can be obtained experimentally via microscopic analysis of tissue specimens. It is important to remark that the modelling of smooth muscle is, so far, not well understood in the literature and its effect is often neglected in existing models.

[1] There are some tests performed *in vivo*, but there are serious ethical issues involved.

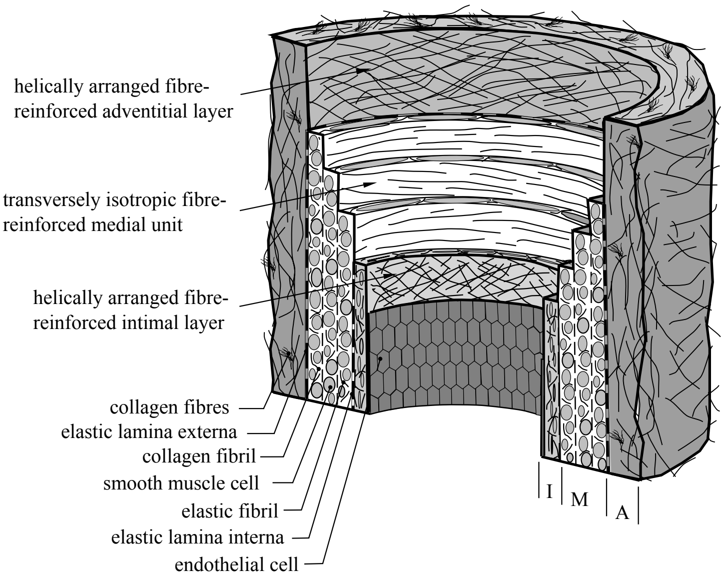

(a) Arterial wall layers (from Holzapfel et al. (2000)).

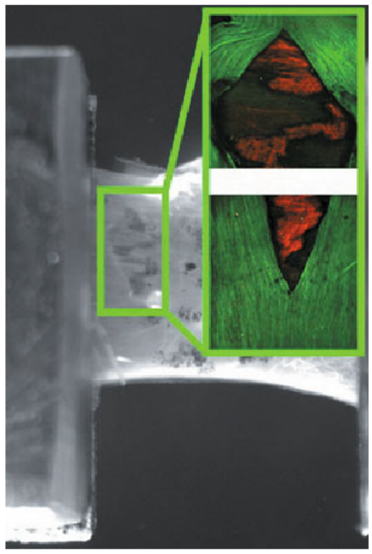

(b) Arterial tissue rupture (from Robertson et al. (2012)).

Figure 1: Illustration and imaging of the arterial wall composition.

3 KINEMATICAL DESCRIPTION

Let $\Omega \subset \mathbb{R}^{\mathrm{nd}}$ be an open set representing a body in the material configuration where the macroscopic problem is defined. At each material point $\mathbf{x} \in \Omega$ we associate a micro-scale domain Ω_μ called RVE (Representative Volume Element) such that $\ell_\mu/\ell \ll 1$, where ℓ_μ and ℓ are characteristics lengths related to the micro-scale and macro-scale respectively. The size ℓ_μ is chosen such that Ω_μ is a representative volume of the material heterogeneities (see Fig. 2). The micro-scale points $\mathbf{y} \in \Omega_\mu$ are referred to a local coordinate system centred in the geometrical centre of the RVE. Thus, by definition, we have $\displaystyle\int_{\Omega_\mu} \mathbf{y}\, d\Omega_\mu = \mathbf{0}$. The gradient operator $\nabla(\cdot)$ is referred to the macro-scale system coordinates, while $\nabla_\mu(\cdot)$ to the micro-scale one.

For simplicity, but without loss of generality, we will not treat explicitly voids or inclusions in this text. However, all the developments presented here can be easily adapted to consider such features.

3.1 Admissible set of micro-scale displacement field

We describe the micro-scale displacement in the RVE, that is $\mathbf{u}_\mu = \mathbf{u}_\mu(\mathbf{y})$ subjected to the two main assumptions:

1. The macro-scale displacement $\mathbf{u} = \mathbf{u}(\mathbf{x})$ is given by the volume average (homogenisation) of the micro-scale displacement field:

$$\mathbf{u}(\mathbf{x}) = \frac{1}{|\Omega_\mu|} \int_{\Omega_\mu} \mathbf{u}_\mu(\mathbf{y})\, d\Omega_\mu \tag{1}$$

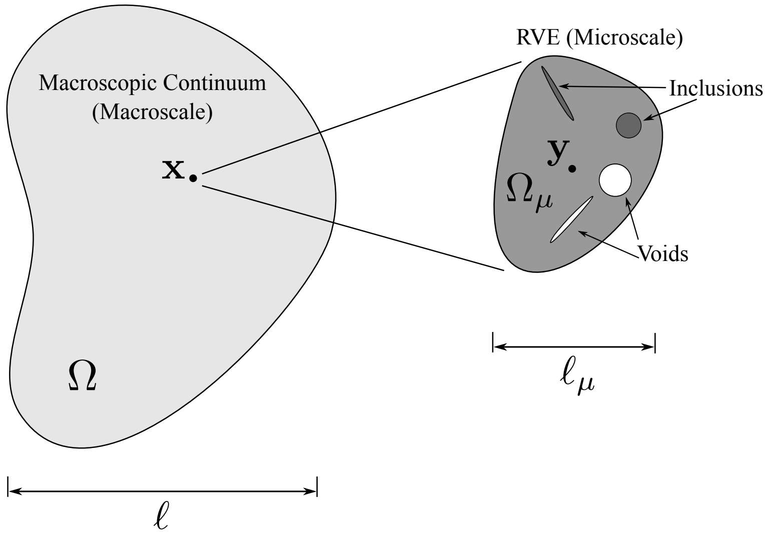

Figure 2: Macro-scale and micro-scale domains.

2. The macro-scale deformation gradient field $\mathbf{F} = \mathbf{F}(\mathbf{x})$ is given by the volume average (homogenisation) of the micro-scale gradient deformation field:

$$\mathbf{F}(\mathbf{x}) = \frac{1}{|\Omega_\mu|} \int_{\Omega_\mu} \mathbf{F}_\mu(\mathbf{y}) \, \mathrm{d}\Omega_\mu \tag{2}$$

where $\mathbf{F}(\mathbf{x}) = \mathbf{I} + \nabla \mathbf{u}(\mathbf{x})$, $\mathbf{F}_\mu(\mathbf{y}) = \mathbf{I} + \nabla_\mu \mathbf{u}_\mu(\mathbf{y})$.

Note that we have used for the macro-scale kinematical descriptors the explicit dependence with the variable $\mathbf{x}$. Throughout the manuscript we will omit this dependence as the point $\mathbf{x} \in \Omega$ is fixed, thus we simply write $\mathbf{u}$ or $\mathbf{F}$. Also we assume that the subscript μ means a micro-scale object (fields depending on $\mathbf{y}$, domains, boundaries, vectors, etc).

Let $\mathscr{U}_\mu$ be a Hilbert space endowed with sufficient regularity for the further mathematical operations. We define $\mathrm{Kin}^*_{\mathbf{u}_\mu} \subset \mathscr{U}_\mu$ as the admissible set of micro-scale displacements as follows:

$$\mathrm{Kin}^*_{\mathbf{u}_\mu} = \left\{ \mathbf{u}_\mu \in \mathscr{U}_\mu; \int_{\Omega_\mu} \mathbf{u}_\mu \, \mathrm{d}\Omega_\mu = |\Omega_\mu| \mathbf{u}; \int_{\Omega_\mu} \mathbf{F}_\mu \, \mathrm{d}\Omega_\mu = |\Omega_\mu| \mathbf{F} \right\} \tag{3}$$

We can also express $\mathbf{u}_\mu$ by means of a Taylor expansion, as a function of macro-scale quantities, $\mathbf{u}$ and $\mathbf{F}$, plus a fluctuation component $\tilde{\mathbf{u}}_\mu(\mathbf{y})$, such that:

$$\mathbf{u}_\mu(\mathbf{y}) = \mathbf{u} + (\mathbf{F} - \mathbf{I})\mathbf{y} + \tilde{\mathbf{u}}_\mu(\mathbf{y}) \tag{4}$$

From (4), the micro-scale deformation gradient yields

$$\mathbf{F}_\mu = \mathbf{I} + \nabla_\mu \mathbf{u}_\mu = \mathbf{F} + \nabla_\mu \tilde{\mathbf{u}}_\mu \tag{5}$$

The expression (4) above shows the decoupled structure of the displacement field involving a uniform component, $\mathbf{u}$, a linear term, $(\mathbf{F} - \mathbf{I})\mathbf{y}$, and a higher order contribution, $\tilde{\mathbf{u}}_\mu$. Making use of such expansion we see that the kinematical constraints in $\mathrm{Kin}^*_{\mathbf{u}_\mu}$ can be fully characterized specifying the kinematical constraints over the fluctuation displacement field $\tilde{\mathbf{u}}_\mu$, as we explain in the next subsection.

3.2 Admissible space of micro-scale fluctuations field

Integrating (4) and (5) over Ω_μ, and taking into account that $\mathbf{u}_\mu \in \mathrm{Kin}^*_{\mathbf{u}_\mu}$ and the origin of $\mathbf{y}$ is at the geometrical centre of the RVE, we have:

$$\int_{\Omega_\mu} \mathbf{u}_\mu \, \mathrm{d}\Omega_\mu = \int_{\Omega_\mu} \mathbf{u} + (\mathbf{F} - \mathbf{I})\mathbf{y} + \tilde{\mathbf{u}}_\mu \, \mathrm{d}\Omega_\mu = |\Omega_\mu|\mathbf{u} + \underbrace{\int_{\Omega_\mu} \tilde{\mathbf{u}}_\mu \, \mathrm{d}\Omega_\mu}_{\text{must be } \mathbf{0}}$$

$$\int_{\Omega_\mu} \mathbf{F}_\mu \, \mathrm{d}\Omega_\mu = \int_{\Omega_\mu} \mathbf{F} + \nabla_\mu \tilde{\mathbf{u}}_\mu \, \mathrm{d}\Omega_\mu = |\Omega_\mu|\mathbf{F} + \underbrace{\int_{\Omega_\mu} \nabla_\mu \tilde{\mathbf{u}}_\mu \, \mathrm{d}\Omega_\mu}_{\text{must be } \mathbf{0}}$$

This leads to the definition:

$$\mathrm{Kin}^*_{\tilde{\mathbf{u}}_\mu} = \left\{ \tilde{\mathbf{u}}_\mu \in \mathscr{U}_\mu; \int_{\Omega_\mu} \tilde{\mathbf{u}}_\mu \, \mathrm{d}\Omega_\mu = \mathbf{0}, \int_{\Gamma_\mu} \nabla_\mu \tilde{\mathbf{u}}_\mu \, \mathrm{d}\Gamma_\mu = \mathbf{0} \right\} \tag{6}$$

Using the classical relation (54) from Appendix A, we have the following equivalent characterization of $\mathrm{Kin}^*_{\tilde{\mathbf{u}}_\mu}$:

$$\mathrm{Kin}^*_{\tilde{\mathbf{u}}_\mu} = \left\{ \tilde{\mathbf{u}}_\mu \in \mathscr{U}_\mu; \int_{\Omega_\mu} \tilde{\mathbf{u}}_\mu \, \mathrm{d}\Omega_\mu = \mathbf{0}, \int_{\Gamma_\mu} \tilde{\mathbf{u}}_\mu \otimes \mathbf{n}_\mu \, \mathrm{d}\Gamma_\mu = \mathbf{0} \right\} \tag{7}$$

where $\mathbf{n}_\mu$ is the unit outward vector normal to the RVE boundary Γ_μ. Let $\mathbf{u}^1_\mu, \mathbf{u}^2_\mu \in \mathrm{Kin}^*_{\mathbf{u}_\mu}$, since both fields satisfy the conditions (1) and (2), the space of admissible fluctuations $\mathrm{Kin}^*_{\tilde{\mathbf{u}}_\mu}$ is identical to the the space of admissible virtual variations $\mathrm{Var}^*_{\mathbf{u}_\mu}$. Using the same argument, the space of admissible virtual variations of fluctuations $\mathrm{Var}^*_{\tilde{\mathbf{u}}_\mu}$ and $\mathrm{Kin}^*_{\tilde{\mathbf{u}}_\mu}$ are also coincident. So we have:

$$\mathrm{Var}^*_{\mathbf{u}_\mu} = \left\{ \hat{\mathbf{u}}_\mu \in \mathscr{U}_\mu; \hat{\mathbf{u}}_\mu = \mathbf{u}^1_\mu - \mathbf{u}^2_\mu \quad, \mathbf{u}^1_\mu \text{ and } \mathbf{u}^2_\mu \in \mathrm{Kin}^*_{\mathbf{u}_\mu} \right\} = \mathrm{Kin}^*_{\tilde{\mathbf{u}}_\mu} = \mathrm{Var}^*_{\tilde{\mathbf{u}}_\mu} \tag{8}$$

Note the use of $\hat{(\cdot)}$ to denote virtual entities. For further developments, it is useful to express the virtual variation $\hat{\mathbf{u}}_\mu$ as a function of the triad $(\hat{\mathbf{u}}, \hat{\mathbf{F}}, \hat{\tilde{\mathbf{u}}}_\mu)$. Taking the variation in (4) and (5) we have:

$$\hat{\mathbf{u}}_\mu = \hat{\mathbf{u}} + \hat{\mathbf{F}}\mathbf{y} + \hat{\tilde{\mathbf{u}}}_\mu \tag{9}$$

$$\hat{\mathbf{F}}_\mu = \hat{\mathbf{F}} + \nabla_\mu \hat{\tilde{\mathbf{u}}}_\mu \tag{10}$$

4 PRINCIPLE OF MULTI-SCALE VIRTUAL POWER

In this section we derive the RVE equilibrium problem and the homogenisation formulae for the stress and body forces. To this aim, the Principle of Multi-scale Virtual Power (PMVP), as proposed in Blanco et al. (2014a,b) and applied in de Souza Neto et al. (2014), is invoked.

The PMVP, which can be understood as a generalized Hill-Mandel Principle of Macrohomogeneity, states that the homogenised total virtual power at the micro-scale is equal to the total virtual power exerted by macroscopic quantities. Thus, the following variational equation must be satisfied:

$$\mathbf{P}\cdot\hat{\mathbf{F}} - \mathbf{b}\cdot\hat{\mathbf{u}} = \frac{1}{|\Omega_\mu|}\int_{\Omega_\mu} \mathbf{P}_\mu\cdot\hat{\mathbf{F}}_\mu - \mathbf{b}_\mu\cdot\hat{\mathbf{u}}_\mu \,\mathrm{d}\Omega_\mu \quad \forall(\hat{\mathbf{u}},\hat{\mathbf{F}},\hat{\tilde{\mathbf{u}}}_\mu)\in\mathbb{R}^{\mathrm{nd}}\times\mathbb{R}^{\mathrm{nd}\times\mathrm{nd}}\times\mathrm{Var}^*_{\tilde{\mathbf{u}}_\mu} \tag{11}$$

where $\mathbf{b}_\mu$ and $\mathbf{P}_\mu$ are the micro-scale body force and the First Piola-Kirchhoff stress tensor with $\mathbf{b}$ and $\mathbf{P}$ their macro-scale counterparts, respectively.

Replacing (9) and (10) into equation (11), and rearranging terms, we have:

$$\begin{aligned}&\left(\int_{\Omega_\mu}\mathbf{b}_\mu\,\mathrm{d}\Omega_\mu - |\Omega_\mu|\mathbf{b}\right)\cdot\hat{\mathbf{u}} + \left(|\Omega_\mu|\mathbf{P} + \int_{\Omega_\mu}\mathbf{b}_\mu\otimes\mathbf{y}\,\mathrm{d}\Omega_\mu - \int_{\Omega_\mu}\mathbf{P}_\mu\,\mathrm{d}\Omega_\mu\right)\cdot\hat{\mathbf{F}} + \\ &+\int_{\Omega_\mu} -\mathbf{P}_\mu\cdot\nabla_\mu\hat{\tilde{\mathbf{u}}}_\mu + \mathbf{b}_\mu\cdot\hat{\tilde{\mathbf{u}}}_\mu = 0 \quad \forall(\hat{\mathbf{u}},\hat{\mathbf{F}},\hat{\tilde{\mathbf{u}}}_\mu)\in\mathbb{R}^{\mathrm{nd}}\times\mathbb{R}^{\mathrm{nd}\times\mathrm{nd}}\times\mathrm{Var}^*_{\tilde{\mathbf{u}}_\mu}\end{aligned} \tag{12}$$

Setting in the first place $\hat{\mathbf{F}} = \mathbf{0}$ and $\hat{\tilde{\mathbf{u}}}_\mu = \mathbf{0}$, and then $\hat{\mathbf{u}} = \hat{\tilde{\mathbf{u}}}_\mu = \mathbf{0}$ in expression (12), we derive two homogenisation procedures for the body force and for the First Piola-Kirchhoff stress tensor, respectively, given by:

$$\mathbf{b} = \frac{1}{|\Omega_\mu|}\int_{\Omega_\mu}\mathbf{b}_\mu\,\mathrm{d}\Omega_\mu \tag{13}$$

$$\mathbf{P} = \frac{1}{|\Omega_\mu|}\left(\int_{\Omega_\mu}\mathbf{P}_\mu\,\mathrm{d}\Omega_\mu - \int_{\Omega_\mu}\mathbf{b}_\mu\otimes\mathbf{y}\,\mathrm{d}\Omega_\mu\right) \tag{14}$$

Note that, differently from what is usually assumed in literature, the homogenisation of the stress is not simply the average of micro-scale stress field.

Finally, setting $\hat{\mathbf{u}} = \mathbf{0}$ and $\hat{\mathbf{F}} = \mathbf{0}$ in (12), the RVE equilibrium problem is obtained: find $\tilde{\mathbf{u}}_\mu \in \mathrm{Kin}^*_{\tilde{\mathbf{u}}_\mu}$ such that

$$\int_{\Omega_\mu}\left[-\mathbf{P}_\mu\cdot\nabla_\mu\hat{\tilde{\mathbf{u}}}_\mu + \mathbf{b}_\mu\cdot\hat{\tilde{\mathbf{u}}}_\mu\right]\mathrm{d}\Omega_\mu = 0 \qquad \forall\hat{\tilde{\mathbf{u}}}_\mu\in\mathrm{Var}^*_{\tilde{\mathbf{u}}_\mu} \tag{15}$$

Integrating by parts the first term in (15) and writing $\mathbf{b}_\mu = \mathbf{b} + \tilde{\mathbf{b}}_\mu$ we have:

$$\int_{\Omega_\mu}(\mathrm{div}\,\mathbf{P}_\mu + \tilde{\mathbf{b}}_\mu)\cdot\hat{\tilde{\mathbf{u}}}_\mu\,\mathrm{d}\Omega_\mu + \int_{\Gamma_\mu}\mathbf{P}_\mu\mathbf{n}_\mu\cdot\hat{\tilde{\mathbf{u}}}_\mu\,\mathrm{d}\Omega_\mu = 0 \qquad \forall\hat{\tilde{\mathbf{u}}}_\mu\in\mathrm{Var}^*_{\tilde{\mathbf{u}}_\mu} \tag{16}$$

Then, as a consequence of the kinematical constraints in the space $\mathrm{Var}^*_{\tilde{\mathbf{u}}_\mu}$, we arrive at the Euler-Lagrange equations as follows:

$$\mathrm{div}\,\mathbf{P}_\mu + \tilde{\mathbf{b}}_\mu = \mathbf{0} \qquad \text{in } \Omega_\mu \tag{17}$$

$$\mathbf{P}_\mu\mathbf{n} = \mathbf{P}\mathbf{n} \qquad \text{on } \Gamma_\mu \tag{18}$$

4.1 Specific subspaces of multi-scale models

So far, the minimally constrained space of admissible fluctuations $\mathrm{Kin}^*_{\tilde{\mathbf{u}}_\mu}$ has been considered. Note that any subspace of $\mathrm{Kin}^*_{\tilde{\mathbf{u}}_\mu}$ could be considered in the analysis. In this sense, we present three different subspaces which fulfill this condition:

1. Taylor model:
$$^T\mathrm{Kin}_{\tilde{\mathbf{u}}_\mu} := \{\mathbf{0}\} \tag{19}$$
2. Linear boundary model:
$$^L\mathrm{Kin}_{\tilde{\mathbf{u}}_\mu} := \{\tilde{\mathbf{u}}_\mu \in \mathrm{Kin}^*_{\tilde{\mathbf{u}}_\mu}; \tilde{\mathbf{u}}_\mu|_{\Gamma_\mu} = \mathbf{0}\} \tag{20}$$
3. Periodic boundary model:
$$^P\mathrm{Kin}_{\tilde{\mathbf{u}}_\mu} := \{\tilde{\mathbf{u}}_\mu \in \mathrm{Kin}^*_{\tilde{\mathbf{u}}_\mu}; \tilde{\mathbf{u}}_\mu|_{\Gamma_\mu^{i,+}} = \tilde{\mathbf{u}}_\mu|_{\Gamma_\mu^{i,-}} \forall i = 1\} \tag{21}$$
where $\Gamma_\mu^{i,+}$ and $\Gamma_\mu^{i,-}$ and $\Gamma_\mu = \bigcup_i \left(\Gamma_\mu^{i,+} \cup \Gamma_\mu^{i,-}\right)$.

In the following sections we use $\mathrm{Kin}_{\tilde{\mathbf{u}}_\mu}$ as a generic set that can be either $^T\mathrm{Kin}_{\tilde{\mathbf{u}}_\mu}$, $^L\mathrm{Kin}_{\tilde{\mathbf{u}}_\mu}$, $^P\mathrm{Kin}_{\tilde{\mathbf{u}}_\mu}$ or $\mathrm{Kin}^*_{\tilde{\mathbf{u}}_\mu}$.

5 MICRO-SCALE EQUILIBRIUM AND LINEARISATION

From now on we consider $\tilde{\boldsymbol{b}}_\mu = \mathbf{0}$. At the micro-scale the problem reduces to find the micro-scale displacement fluctuation field $\tilde{\mathbf{u}}_\mu$ induced by the insertion of macro-scale deformation gradient, $\mathbf{F}$, into the RVE domain. Thus the micro-scale mechanical problem can be enunciated as: Given $\mathbf{F} \in \mathbb{R}^{\mathrm{nd}\times\mathrm{nd}}$ a known deformation gradient (from the macro-scale), find $\tilde{\mathbf{u}}_\mu \in \mathrm{Kin}_{\tilde{\mathbf{u}}_\mu}$ such that:

$$\int_{\Omega_\mu} \mathbf{P}_\mu(\mathbf{F} + \nabla\tilde{\mathbf{u}}_\mu) \cdot \nabla\hat{\tilde{\mathbf{u}}}_\mu \, d\Omega_\mu = 0 \qquad \forall \hat{\tilde{\mathbf{u}}}_\mu \in \mathrm{Var}_{\tilde{\mathbf{u}}_\mu} \tag{22}$$

where

$$\mathbf{P}_\mu = \mathbf{F}_\mu\mathbf{S}_\mu = (\mathbf{F} + \nabla\tilde{\mathbf{u}}_\mu)\,\mathbf{S}_\mu, \tag{23}$$

with

$$\mathbf{S}_\mu = 2\frac{\partial\Psi(\mathbf{C}_\mu)}{\partial\mathbf{C}_\mu}, \tag{24}$$

and recalling that $\mathbf{C}_\mu = \mathbf{F}_\mu^T\mathbf{F}_\mu = (\mathbf{F} + \nabla\tilde{\mathbf{u}}_\mu)^T(\mathbf{F} + \nabla\tilde{\mathbf{u}}_\mu)$ and $\Psi(\mathbf{C}_\mu)$ is a given strain energy function .

For the purposes of this work, we consider Ψ defined as the sum of Ψ^{iso} from a neo-hookean model and Ψ^{vol} from a volumetric energy function, as follows (see Holzapfel (2000)):

$$\begin{aligned}\Psi(\mathbf{C}_\mu) &= \Psi^{iso}(I_1(\overline{\mathbf{C}}_\mu)) + \Psi^{vol}(J_\mu)\\ &= \frac{c}{2}(I_1(\overline{\mathbf{C}}_\mu) - 3) + \frac{\kappa}{2}(J_\mu^2 - 1 - 2\log J_\mu)\end{aligned} \tag{25}$$

where c and κ are material parameters, $J_\mu = \det \mathbf{F}_\mu$, $\overline{\mathbf{C}}_\mu = J_\mu^{-2/3}\mathbf{C}_\mu$ is the isochoric counterpart of $\mathbf{C}_\mu$ and $I_1(\overline{\mathbf{C}}_\mu) = \mathrm{tr}\,\overline{\mathbf{C}}_\mu$.

In order to solve the micro-scale equilibrium problem by using the Newton-Raphson scheme (see Appendix A), we take the Gâteaux derivative of $\mathbf{P}_\mu(\mathbf{F}_\mu)$, and then we define the micro-scale tangent fourth-order tensor as:

$$\delta\mathbf{P}_\mu(\mathbf{F}_\mu, \delta\mathbf{F}_\mu) = \mathbb{D}_\mu(\mathbf{F}_\mu)\delta\mathbf{F}_\mu = \mathbb{D}_\mu(\mathbf{F}_\mu)\nabla_\mu\delta\tilde{\mathbf{u}}_\mu \tag{26}$$

with the following Cartesian components:

$$(\mathbb{D}_\mu)_{ijkl} = \left[\frac{\partial\mathbf{P}_\mu}{\partial\mathbf{F}_\mu}\right]_{ijkl} = \frac{\partial(\mathbf{P}_\mu)_{ij}}{\partial(\mathbf{F}_\mu)_{kl}} \tag{27}$$

or in terms of strain-energy:

$$(\mathbb{D}_\mu)_{ijkl} = \left[\frac{\partial^2\Psi}{\partial\mathbf{F}_\mu\partial\mathbf{F}_\mu}\right]_{ijkl} = \frac{\partial^2\Psi}{\partial(\mathbf{F}_\mu)_{ij}\partial(\mathbf{F}_\mu)_{kl}} \tag{28}$$

It is also useful to express $\mathbb{D}_\mu$ in terms of the symmetric tensors ($\mathbf{S}_\mu$,$\mathbf{C}_\mu$), so we have:

$$(\mathbb{D}_\mu)_{ijkl} = \left[2\frac{\partial\mathbf{S}_\mu}{\partial\mathbf{C}_\mu}\right]_{njml}(\mathbf{F}_\mu)_{km}(\mathbf{F}_\mu)_{in} + (\mathbf{S}_\mu)_{lj}\delta_{ki} \tag{29}$$

Hence, the linearised RVE equilibrium problem can be written as follows: Given $\tilde{\mathbf{u}}_\mu^k \in \mathrm{Kin}_{\tilde{\mathbf{u}}_\mu}$ and $\mathbf{F}_\mu^k = \mathbf{F} + \nabla_\mu\tilde{\mathbf{u}}_\mu^k$, find $\delta\tilde{\mathbf{u}}_\mu^k \in \mathrm{Var}_{\tilde{\mathbf{u}}_\mu}$ such that:

$$\int_{\Omega_\mu}\mathbb{D}_\mu(\mathbf{F}_\mu^k)\nabla_\mu\delta\tilde{\mathbf{u}}_\mu^k\cdot\nabla\hat{\tilde{\mathbf{u}}}_\mu\,\mathrm{d}\Omega_m = -\int_{\Omega_\mu}\mathbf{P}_\mu(\mathbf{F}_\mu^k)\cdot\nabla\hat{\tilde{\mathbf{u}}}_\mu\,\mathrm{d}\Omega_\mu \qquad \forall\hat{\tilde{\mathbf{u}}}_\mu \in \mathrm{Var}_{\tilde{\mathbf{u}}_\mu} \tag{30}$$

then perform the increment of $\tilde{\mathbf{u}}_\mu$ for the next iteration as

$$\tilde{\mathbf{u}}_\mu^{k+1} = \tilde{\mathbf{u}}_\mu^k + \delta\tilde{\mathbf{u}}_\mu^k \tag{31}$$

until a convergence criteria is achieved.

6 DAMAGE MODELLING

Following the works Simo (1987) and Simo and Ju (1987) we introduce the notion of damage surface $\Phi = 0$ through the function:

$$\Phi(\mathbf{F}_\mu, r) = \sqrt{2\Psi^0(\mathbf{F}_\mu)} - r \leq 0 \tag{32}$$

where Ψ^0 is the strain-energy of the undamaged material and r is a strain-like internal variable with a minimum threshold r_0 which rules the size of the elastic domain. The evolution of r is such that, for a given pseudo-time t, we have:

$$r(t) = \max_{s\in[0,t]}\left\{r_0, \sqrt{2\Psi^0(\mathbf{F}_\mu(s))}\right\} \tag{33}$$

We can also define a stress-like internal variable, q, whose rate is expressed as:

$$\dot{q} = H(r)\dot{r} \tag{34}$$

where, if $H > 0$ there is strain hardening, while if $H < 0$ there is strain softening. Both, q and r, have the same initial value denoted as $q(t = 0) = q_0 = r_0$. The damage variable is defined as:

$$d = 1 - \frac{q(r)}{r} \tag{35}$$

The damaged strain-energy is then given by:

$$\Psi(\mathbf{F}_\mu, d) = (1 - d)\Psi^0(\mathbf{F}_\mu) \tag{36}$$

and the damaged first Piola-Kirchhoff stress tensor:

$$\mathbf{P}_\mu = (1 - d)\frac{\partial \Psi^0}{\partial \mathbf{F}_\mu} = (1 - d)\mathbf{P}^0_\mu \tag{37}$$

Denoting $\mathbb{D}^0_\mu(\mathbf{F}_\mu) = \dfrac{\partial \mathbf{P}^0_\mu}{\partial \mathbf{F}_\mu}$ it can be shown that the damaged tangent tensor is given by:

$$\mathbb{D}_\mu(\mathbf{F}_\mu, d) = \begin{cases} (1 - d)\mathbb{D}^0_\mu(\mathbf{F}_\mu) & \dot{r} = 0 \\ (1 - d)\mathbb{D}^0_\mu(\mathbf{F}_\mu) - \left(\dfrac{q - H(r)r}{r^3}\right)\mathbf{P}^0_\mu \otimes \mathbf{P}^0_\mu & \dot{r} > 0 \end{cases} \tag{38}$$

Alternative damage criteria can be found in Miehe (1995) and Blanco et al. (2015). In this work we consider a regularized softening function proposed in Toro et al. (2016), which is given below:

$$H(r) = H_0 \exp\left[H_0\left(\frac{r - r_0}{r_0}\right)\right], \qquad H_0 = -\frac{r_0^2 \ell_\mu}{G_f} \tag{39}$$

where G_f is the fracture energy released during the failure and ℓ_μ is a characteristic length (in the context of finite element method, ℓ_μ is the characteristic size of the element). The term regularized refers to the consideration of the parameter ℓ_μ in order to guarantee a consistent total dissipation of the fracture energy G_f. For further explanation and additional details see Oliver (1989).

There are others possibilities for modelling damage in the biomechanics field. One is the so-called *Pseudoelasticity* approach (Ogden and Roxburgh, 1999), where an additional function depending on the damage is added on the strain energy function. Users of this methodology claim some advantages with respect to the experimental calibration of materials parameters (Weisbecker et al., 2012; Dorfmann and Ogden, 2004; Peña and Doblaré, 2009). A comparison between pseudoelasticity and classical continuum damage models can be found in Gracia et al. (2009).

Some efforts have also been made on the collagenous tissues damage modelling in Balzani et al. (2012) and Schmidt et al. (2014). The last one introduces a statistical distribution to characterize the collagen fibres degradation. In this context, a multi-scale approach can be found in Hadi et al. (2012).

There are also degradation processes where damage evolves even in unloading regions. However, this phenomenology has not been considered in the present work.

7 TANGENT HOMOGENISATION AND MACRO-SCALE BIFURCATION ANALYSIS

In a nonlinear multi-scale analysis, the linearisation of the homogenisation formulae is fundamental for the solution of the macro-scale nonlinear equations through any gradient-based method (such as the Newton-Raphson method). In the case of materials which undergo degradation and failure, the calculation of the tangent operator also provides further insight about the mechanical state of the structure, in fact, it makes possible to carry out a bifurcation analysis.

Following the work of de Souza Neto and Feijóo (2006), we define the homogenised tangent tensor as the derivative of the homogenised Piola-Kirchhoff stress tensor $\mathbf{P}$ with respect to the macro-scale deformation gradient $\mathbf{F}$, that is:

$$\mathbb{D}(\mathbf{F}) := \frac{\partial \mathbf{P}(\mathbf{F})}{\partial \mathbf{F}} \tag{40}$$

It can be proved that two terms contribute to the homogenised tangent operator:

$$\mathbb{D} = \overline{\mathbb{D}} + \widetilde{\mathbb{D}} \tag{41}$$

where $\overline{\mathbb{D}}$ is the so-called Taylor contribution given by:

$$\overline{\mathbb{D}}(\mathbf{F}) = \frac{1}{|\Omega_\mu|} \int_{\Omega_\mu} \mathbb{D}_\mu(\mathbf{F}_\mu)\, \mathrm{d}\Omega_\mu \tag{42}$$

$\mathbb{D}_\mu(\mathbf{F}_\mu)$ being the micro-scale tangent tensor, obtained from (38), and $\widetilde{\mathbb{D}}$ is the fluctuation component given by

$$\widetilde{\mathbb{D}}(\mathbf{F}) = \left[\frac{1}{|\Omega_\mu|} \int_{\Omega_\mu} (\mathbb{D}_\mu(\mathbf{F}_\mu))_{ijpq} \left(\nabla_\mu \Delta \tilde{\mathbf{u}}_{kl}\right)_{pq} \mathrm{d}\Omega_\mu \right] \mathbf{e}_i \otimes \mathbf{e}_j \otimes \mathbf{e}_k \otimes \mathbf{e}_l \tag{43}$$

where $\Delta\tilde{\mathbf{u}}_{kl}$, $k, l = 1, \ldots, \mathrm{nd}$, are the solutions of the following canonical problem: given $\mathbf{F}_\mu$, find $\Delta\tilde{\mathbf{u}}_{kl}$ such that:

$$\int_{\Omega_\mu} \mathbb{D}_\mu(\mathbf{F}_\mu) \nabla_\mu \Delta\tilde{\mathbf{u}}_{kl} \cdot \nabla_\mu \hat{\tilde{\mathbf{u}}}_\mu \, \mathrm{d}\Omega_\mu = -\int_{\Omega_\mu} \mathbb{D}_\mu(\mathbf{F}_\mu)(\mathbf{e}_k \otimes \mathbf{e}_l) \cdot \nabla_\mu \hat{\tilde{\mathbf{u}}}_\mu \, \mathrm{d}\Omega_\mu \qquad \forall \hat{\tilde{\mathbf{u}}}_\mu \in \mathrm{Var}_{\tilde{\mathbf{u}}_\mu} \tag{44}$$

In Appendix B, the reader can find additional details about the present derivations.

Now we are able to define the so-called *localization tensor* or *acoustic tensor* $\mathbf{Q}$ (Rice, 1976). The spectral properties of this tensor give us information about the nucleation time and orientation of strain-localization bands. By considering the Maxwell's kinematical compatibility condition, a discontinuity of the deformation gradient rate should have the following tensor structure [2]:

$$[\![\dot{\mathbf{F}}]\!] = \dot{\boldsymbol{\gamma}} \otimes \mathbf{n} \tag{45}$$

[2]Note that given a surface S with normal $\mathbf{n}$ we denote $[\![(\cdot)]\!] = (\cdot)|_{(\mathbf{x}+\mathrm{d}\mathbf{x})} - (\cdot)|_{(\mathbf{x}-\mathrm{d}\mathbf{x})} \forall \mathbf{x} \in S$ with $\mathrm{d}\mathbf{x}$ parallel to the $\mathbf{n}$-direction and $\|\mathrm{d}\mathbf{x}\| \to 0$

where $\dot{\boldsymbol{\gamma}}$ denotes the initial jump rate direction and $\mathbf{n}$ is the direction of the vector normal to the localization band. Enforcing the traction continuity between the stress state of a point inside the strain localization band and another point outside the band, we arrive at the definition of the localization tensor $\mathbf{Q}(\mathbf{F}, \mathbf{n})$ at the bifurcation time as:

$$[\![\dot{\mathbf{P}}\mathbf{n}]\!] = [\![\mathbb{D}(\mathbf{F})\dot{\mathbf{F}}]\!]\mathbf{n} = (\mathbb{D}(\mathbf{F})\dot{\boldsymbol{\gamma}} \otimes \mathbf{n})\mathbf{n} := \mathbf{Q}(\mathbf{F}, \mathbf{n})\dot{\boldsymbol{\gamma}} = \mathbf{0} \qquad \forall \dot{\boldsymbol{\gamma}} \tag{46}$$

or in Cartesian components:

$$(\mathbf{Q})_{ik} = (\mathbb{D})_{ijkl}(\mathbf{n})_j(\mathbf{n})_l \tag{47}$$

Non-trivial solutions of (46), i.e. $\dot{\boldsymbol{\gamma}} \neq \mathbf{0}$, require that:

$$\det \mathbf{Q}(\mathbf{F}, \mathbf{n}) = 0 \tag{48}$$

Condition (48) is used in this work to determine macro-scale bifurcation, i.e. the nucleation time and the orientation of a macro-scale discontinuous mode.

8 NUMERICAL EXAMPLES

In this example, we analyse three RVEs with different sizes but with identical micro-structure, which consists of an elastic material matrix and inclined bands characterized by a material that can develop damage. The first RVE is the unit square with a inclined band of $\theta^* = 0.29\,\mathrm{rad} = 16.7^o$. The second and third RVEs are the unit square repeated vertically two and three times, respectively, as seen in Fig. 3. In each RVE, only one band is allowed to degrade enabling damage evolution.

We impose a macro-scale deformation gradient, $\mathbf{F}$, which induces a Mode I of fracture in the RVE:

$$\mathbf{F} = \mathbf{I} + \lambda \mathbf{n} \otimes \mathbf{n} \tag{49}$$

where $\lambda \in [0.0, 0.6]$ is a scalar parameter defining magnitude of the stretch and $\mathbf{n} = (\cos\theta, \mathrm{sen}\,\theta)$ is a unit vector normal to the band such that $\theta = \pi/2 + \theta^*$ (see Fig. 3).

The elastic regime is modelled using a compressible neo-hookean model as in (25) with $c = 800$ and $\kappa = 10000$ [3]. The parameters for the damage model (39) are $H_0 = -0.005, r_0 = 5.0$.

All RVEs are subjected to the following boundary conditions: minimal kinematical constraints (as given by the space $\mathrm{Var}_{\tilde{\mathbf{u}}_\mu}$) and a rotated periodicity condition aligned with the damaged band. Thus, for example, the kinematical admissible space for displacement fluctuations related to the RVE1 is:

$$\mathrm{Kin}_{\tilde{\mathbf{u}}_\mu} = \{\tilde{\mathbf{u}}_\mu \in \mathrm{Kin}^*_{\tilde{\mathbf{u}}_\mu}; \tilde{\mathbf{u}}_\mu(p_1^+) = \tilde{\mathbf{u}}_\mu(p_1^-), \tilde{\mathbf{u}}_\mu(p_2^+) = \tilde{\mathbf{u}}_\mu(p_2^-)\} \tag{50}$$

This boundary condition is imposed to promote the localization pattern in a pure Mode I. In order to eliminate rigid motions, the displacement fluctuation is fixed to zero on the left-bottom vertex.The second and third RVE have analogous boundary conditions.

[3] In these examples all the units are omitted for the sake of simplicity

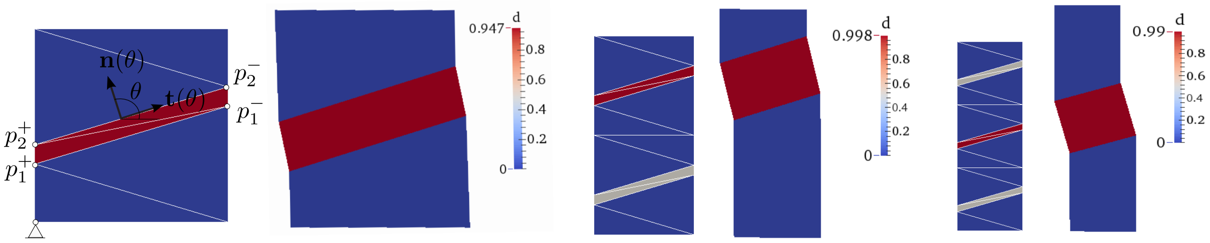

Figure 3: Physical and finite element simulation results for the 3 settings of RVEs.

Fig. 4(a) shows the homogenized stress vs. stretch curve in terms of the normal component of traction, that is $\mathbf{P}_{nn} = (\mathbf{Pn}) \cdot \mathbf{n}$. It is clearly observed that after the curve reaches a peak load, the homogenized material response becomes strongly sensitive to the RVE-size. After crossing the limit stress, the multi-scale model loses objectivity with respect to the RVE-size (Sánchez et al., 2013; Toro et al., 2016). This issue is a direct consequence of the well-know size effect phenomenon, inherent to fracture mechanics problems. As we see in Fig. 4(a), the macro-scale bifurcation analysis results in a reliable technique to determine the point (or pseudo-time) where the macro-scale response loses objectivity. This criterion also gives us the correct information about the orientation of a strain localization band that is being induced at the macro-scale, see Fig. 4(c). On the other hand, Fig. 4(b) depicts the tangent component of stress, $\mathbf{P}_{nt} = (\mathbf{Pn}) \cdot \mathbf{t}$, as a function of the stretch magnitude λ. The same effect related to the lack of objectivity is observed after macro-scale bifurcation.

The previous results clearly show that a reformulation of the classical multiscale model is required after macro-scale bifurcation to address the multi-scale modelling in the postcritical regime, see for example Sánchez et al. (2013); Toro et al. (2016).

Motivated by microscopical images from the Intima tissue (Fig. 5(a)) where a porous microstructure is shown we consider a more complicated example with two porous RVEs as in Fig. 6(a) and Fig. 6(c). They are composed of 9 pores with equal size and have 10% of porosity, the first RVE has all the pores circular and structurally while the other RVE is composed with elliptic pores with 1.3 of eccentricity which are randomly placed and inclined.

We apply an horizontal axial macro deformation gradient as follows

$$\mathbf{F} = \mathbf{I} + \lambda \mathbf{e}_1 \otimes \mathbf{e}_1 \tag{51}$$

varying $\lambda \in [0.0, 0.25]$ in 20 loading steps. We use the same material model and parameters as in the first example. For the damage evolution we use $r_0 = 5$ and $H_0 = -0.025$.

We can see in the Fig. 5(b) that the random RVE localizes first and with a smaller maximum stress compared to the structured case. These localization bands can be seen on Fig. 6(b) and 6(d). It can be seen that the band tends to propagates between the nearest pores and on the major principal directions in the case of elipses, such that the localization bands are easier to propagates in the eliptical pores RVE example, explaining somehow the results of Fig. 5(b).

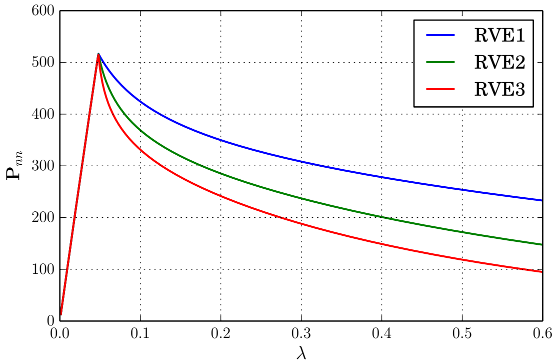

(a) Homogenised normal projection of the traction.

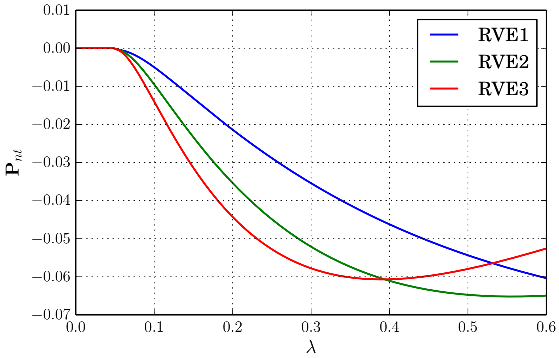

(b) Homogenised tangent projection of the traction.

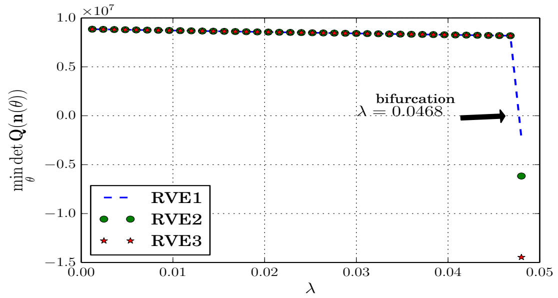

(c) Minimum determinant of the localization tensor as a function of stretch parameter.

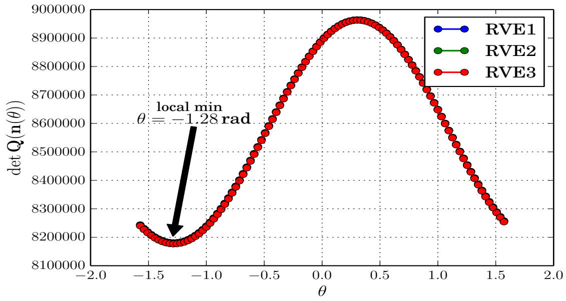

(d) Curve for $\det \mathbf{Q}$ one step before bifurcation.

Figure 4: Results provided from the macro-scale bifurcation analysis.

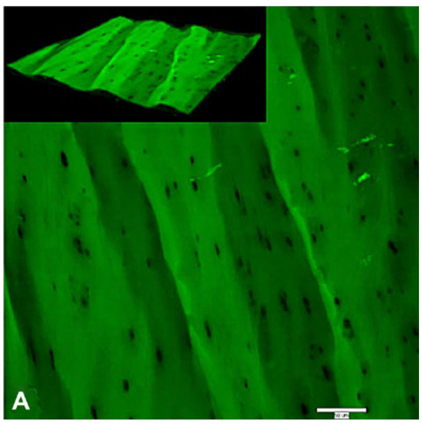

(a) Intima lamina (from Robertson et al. (2012)).

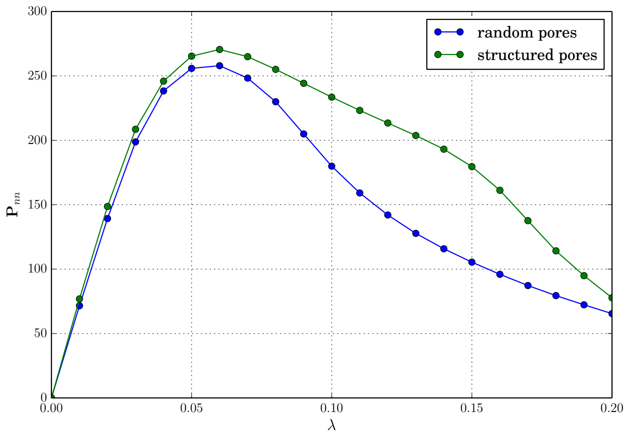

(b) Homogenised Piola-Kirchhoff stress curves.

Figure 5: Porous RVEs motivation and analysis.

9 FINAL REMARKS

Following an axiomatic approach posed in a variational setting, we have presented the foundations of the multi-scale modelling of solid materials in the finite strain regime. As

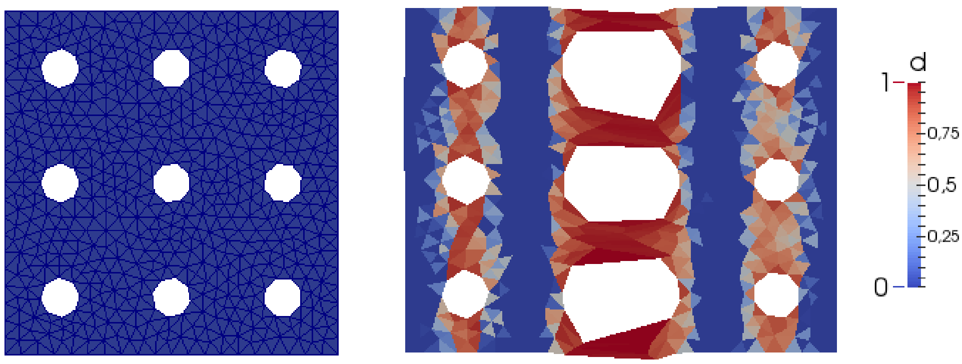

(a) Underformed mesh with 9 circular pores structurally distributed (1090 triangles).

(b) Deformed configuration and damage of Fig. 6(a) after loading.

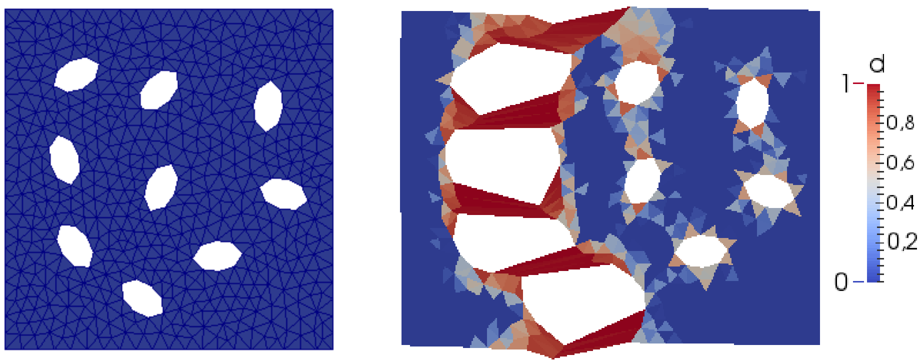

(c) Underformed mesh with 9 elliptic pores randomly distributed (1032 triangles).

(d) Deformed configuration and damage of Fig. 6(c) after loading.

Figure 6: Porous RVEs meshes.

basic assumptions we have postulated (i) the homogenisation of the displacement vector and of the deformation gradient tensor as volume average of the microscopic quantities inside the RVE and (ii) a Principle of Multiscale Virtual Power. As a consequence, homogenisation formulae for the body force and for the Piola-Kirchhoff stress tensor were consistently derived.

This theoretical framework was employed to address the modeling of arterial tissues, in which micro-scale degradation mechanisms take place yielding, ultimately, a critical point is reached in which macro-scale material failure occurs. The identification of this critical point is driven by the analysis of the acoustic tensor, related to the macro-scale tangent operator obtained from the homogenisation procedure. Preliminary results show that this modeling approach allows to identify at the macro-scale the appearing of degradation phenomena from micro-scale failure mechanisms. These results are promising towards a rational modeling of the rupture phenomena in arterial tissues.

ACKNOWLEDGEMENTS

F. Rocha, P.J. Blanco and R.A. Feijóo acknowledge the financial support from the Brazilian agencies CNPq and FAPERJ. P.J. Sanchez and A.E. Huespe acknowledge the financial support from CONICET (grant PIP 2013-2015 631) and from the European Research Council under the European Unions Seventh Framework Programme (FP/2007-2013)/ERC Grant Agreement N. 320815 (ERC Advanced Grant Project Advanced tools for computational design of engineering materials COMPDES-MAT).

References

Balzani, D., Brinkhues, S., and Holzapfel, G. A. (2012). Constitutive framework for the modeling of damage in collagenous soft tissues with application to arterial walls. *Computer Methods in Applied Mechanics and Engineering*, 213–216(0):139 – 151. 10

Blanco, P. J., Sánchez, P. J., de Souza Neto, E. A., and Feijóo, R. A. (2014a). Variational foundations and generalized unified theory of rve-based multiscale models. *Archives of Computational Methods in Engineering*, pages 1–63. 2, 6

Blanco, P. J., Sánchez, P. J., de Souza Neto, E. A., and Feijóo, R. A. (2014b). Variational foundations of rve-based multiscale models. *LNCC Research and Development Internal Report*. 2, 6

Blanco, S., Polindara, C. A., and Goicolea, J. M. (2015). A regularised continuum damage model based on the mesoscopic scale for soft tissue. *International Journal of Solids and Structures*, 58:20 – 33. 10

de Souza Neto, E., Blanco, P., Sánchez, P., and Feijóo, R. (2014). An rve-based mutiscale theory of solids with micro-scale inertia and body force effects. *Mechanics of Materials*. 6

de Souza Neto, E. and Feijóo, R. (2006). Variational foundation of multi-scale constitutive models of solids: small and large strain kinematical formulation. *LNCC Research and Development Report*. 2, 11

de Souza Neto, E. and Feijóo, R. (2008). On the equivalence between spatial and material volume averaging of stress in large strain multi-scale solid constitutive models. *Mechanics of Materials*, 40(10):803–811. 2

Dorfmann, A. and Ogden, R. (2004). A constitutive model for the mullins effect with permanent set in particle-reinforced rubber. *International Journal of Solids and Structures*, 41(7):1855–1878. cited By (since 1996)156. 10

Gracia, L., Peña, E., Royo, J., Pelegay, J., and Calvo, B. (2009). A comparison between pseudo-elastic and damage models for modelling the mullins effect in industrial rubber components. *Mechanics Research Communications*, 36(7):769–776. cited By (since 1996)0. 10

Hadi, M., Sander, E., and Barocas, V. (2012). Multiscale model predicts tissue-level failure from collagen fiber-level damage. *Journal of Biomechanical Engineering*, 134(9). cited By (since 1996)8. 10

Heidenreich, P. A., Trogdon, J. G., Khavjou, O. A., Butler, K., Dracup, J., Ezekowitz, M., Finkelstein, E. A., Hong, Y., Johnston, A. L.-J. D., Khera, S. C., Nelson, S. A., Nichol, D., Orenstein, G., Wilson, P. W., and Woo., Y. J. (2011). Forecasting the future of cardiovascular disease in the united states: A policy statement from the american heart association. *Circulation*, 123(8):933–944. 2

Hill, R. (1965). A self-consistent mechanics of composite materials. *Journal of the Mechanics and Physics of Solids*, 13(4):213 – 222. 2

Holzapfel, G., Gasser, T., and Ogden, R. (2000). A new constitutive framework for arterial wall mechanics and a comparative study of material models. *Journal of Elasticity*, 61(1-3):1–48. 4

Holzapfel, G. A. (2000). *Nonlinear Solid Mechanics. A continuum Approach for Engineering.* London : John Wiley Sons. 8

Mendis, S. (2011). Global atlas on cardiovascular disease prevention and control. *World Health Organization*, pages chapter 1,page 155. 2

Miehe, C. (1995). Discontinuous and continuous damage evolution in Ogden-type large-strain elastic materials. *Eur. J. Mech. A/Solids*, 14(5):697–720. 10

Ogden, R. and Roxburgh, D. (1999). A pseudo-elastic model for the mullins effect in filled rubber. *Proceedings of the Royal Society A: Mathematical, Physical and Engineering Sciences*, 455(1988):2861–2877. cited By (since 1996)220. 10

Oliver, J. (1989). A consistent characteristic length for smeared cracking models. *International Journal for Numerical Methods in Engineering*, 28(2):461–474. 10

Peña, E. and Doblaré, M. (2009). An anisotropic pseudo-elastic approach for modelling mullins effect in fibrous biological materials. *Mechanics Research Communications*, 36(7):784–790. cited By (since 1996)24. 10

Rice, J. R. (1976). The localization of plastic deformation. In *in: W.T. Koiter (Ed.), Theoretical and Applied Mechanics*, pages 207–220. North-Holland Publishing Company. 11

Robertson, A., Hill, M., and Li, D. (2012). Structurally motivated damage models for arterial walls. theory and application. *D. Ambrosi, A. Quarteroni, G. Rozza (Eds.), Modelling of Physiological Flows, Simulation and Applications*, 5:143–185. 4, 14

Schmidt, T., Balzani, D., and Holzapfel, G. A. (2014). Statistical approach for a continuum description of damage evolution in soft collagenous tissues. *Computer Methods in Applied Mechanics and Engineering*, 278(0):41 – 61. 10

Simo, J. (1987). On a fully three-dimensional finite-strain viscoelastic damage model: Formulation and computational aspects. *Computer Methods in Applied Mechanics and Engineering*, 60(2):153–173. cited By (since 1996)374. 9

Simo, J. and Ju, J. (1987). Strain- and stress-based continuum damage models—i. formulation. *International Journal of Solids and Structures*, 23(7):821 – 840. 9

Speirs, D. C. D., de Souza Neto, E. A., and Perić, D. (2008). An approach to the mechanical constitutive modelling of arterial tissue based on homogenization and optimization. *J Biomech*, 41(12):2673–80. 2

Sánchez, P., Blanco, P., Huespe, A., and Feijóo, R. (2013). Failure-oriented multi-scale variational formulation: Micro-structures with nucleation and evolution of softening bands. *Computer Methods in Applied Mechanics and Engineering*, 257(0):221 – 247. 3, 13

Toro, S., Sánchez, P., Blanco, P., de Souza Neto, E., Huespe, A., and Feijóo, R. (2016). Multiscale formulation for material failure accounting for cohesive cracks at the macro and micro scales. *International Journal of Plasticity*, 76:75 – 110. 10, 13

Weisbecker, H., Pierce, D. M., Regitnig, P., and Holzapfel, G. A. (2012). Layer-specific damage experiments and modeling of human thoracic and abdominal aortas with non-atherosclerotic intimal thickening. *Journal of the Mechanical Behavior of Biomedical Materials*, 12(0):93 – 106. 10

A Useful Formulae

Some classical tensor identities are reviewed here:

$$\int_\Omega \operatorname{div} \mathbf{S} \, \mathrm{d}\Omega_\mu = \int_\Gamma \mathbf{S}\mathbf{n} \, \mathrm{d}\Gamma \tag{52}$$

$$\int_\Omega \nabla\phi \, \mathrm{d}\Omega_\mu = \int_\Gamma \phi\mathbf{n} \, \mathrm{d}\Gamma \tag{53}$$

$$\int_\Omega \nabla\mathbf{v} \, \mathrm{d}\Omega_\mu = \int_\Gamma \mathbf{v}\otimes\mathbf{n} \, \mathrm{d}\Gamma \tag{54}$$

$$\int_\Omega \mathbf{S}(\nabla\mathbf{v})^T \, \mathrm{d}\Omega_\mu = -\int_\Omega \operatorname{div} \mathbf{S}\otimes\mathbf{v} \, \mathrm{d}\Omega_\mu + \int_\Gamma \mathbf{S}\mathbf{n}\otimes\mathbf{v} \, \mathrm{d}\Gamma \tag{55}$$

where Ω represents an arbitrary open/bounded domain with piece-wise smooth boundary Γ, $\mathbf{n}$ is the (outward) unit vector normal to Γ, while ϕ, $\mathbf{v}$ and $\mathbf{S}$ are sufficiently smooth scalar, vector and second order tensor fields, respectively (the term suffciently smooth refers to regularity requirements such that previous expressions preserve mathematical sense).

A generally nonlinear variational problem amounts to find $\mathbf{u} \in \mathscr{U}$ such that:

$$\langle \mathcal{R}(\mathbf{u}), \hat{\mathbf{u}} \rangle = 0 \qquad \forall \hat{\mathbf{u}} \in \mathscr{V} \tag{56}$$

where $\mathcal{R} : \mathscr{U} \mapsto \mathscr{V}'$ and $\langle \cdot, \cdot \rangle$ is a bilinear form in the space $\mathscr{V}' \times \mathscr{V}$. The Newton-Raphson method consists in solving iteratively the problem: Given $\mathbf{u}^{(k)} \in \mathscr{U}$, find $\delta\mathbf{u}^{(k)} \in \mathscr{V}$ such that:

$$\langle \delta\mathcal{R}(\mathbf{u}^{(k)}, \delta\mathbf{u}^{(k)}), \hat{\mathbf{u}} \rangle = -\langle \mathcal{R}(\mathbf{u}^{(k)}), \hat{\mathbf{u}} \rangle \qquad \forall \hat{\mathbf{u}} \in \mathscr{V} \tag{57}$$

then, update for the next iteration as

$$\mathbf{u}^{(k+1)} = \mathbf{u}^{(k)} + \delta\mathbf{u}^{(k)} \tag{58}$$

until a convergence criteria is achieved.

B Derivation of the homogenised tangent

Following the definition (40) and considering a perturbation in the component $(\mathbf{F})_{kl}$ we have:

$$\mathbb{D}(\mathbf{F}) = \frac{\partial \mathbf{P}(\mathbf{F})}{\partial \mathbf{F}} = \lim_{\varepsilon \to 0} \frac{1}{\varepsilon} \left[\mathbf{P}(\mathbf{F} + \varepsilon \mathbf{e}_k \otimes \mathbf{e}_l) - \mathbf{P}(\mathbf{F})\right]_{ij} \, \mathbf{e}_i \otimes \mathbf{e}_j \otimes \mathbf{e}_k \otimes \mathbf{e}_l \tag{59}$$

Being $\tilde{\mathbf{u}}_\mu^{kl,\varepsilon} \in \mathrm{Kin}_{\tilde{\mathbf{u}}_\mu}$ the solution of the perturbed micro-scale fluctuation problem as follows:

$$\int_{\Omega_\mu} \mathbf{P}_\mu(\mathbf{F} + \varepsilon \mathbf{e}_k \otimes \mathbf{e}_l + \nabla_\mu \tilde{\mathbf{u}}_\mu^{kl,\varepsilon}) \cdot \nabla_\mu \hat{\tilde{\mathbf{u}}}_\mu \, \mathrm{d}\Omega_\mu = 0 \qquad \forall \hat{\tilde{\mathbf{u}}}_\mu \in \mathrm{Var}_{\tilde{\mathbf{u}}_\mu} \tag{60}$$

Defining $\Delta \tilde{\mathbf{u}}_{kl}^\varepsilon$ through the relation:

$$\tilde{\mathbf{u}}_\mu^{kl,\varepsilon} = \tilde{\mathbf{u}}_\mu + \Delta \tilde{\mathbf{u}}_{kl}^\varepsilon \tag{61}$$

We have expanding (60) by Taylor series

$$\int_{\Omega_\mu} \mathbf{P}_\mu(\mathbf{F}_\mu + \varepsilon \mathbf{e}_k \otimes \mathbf{e}_l + \nabla_\mu \Delta \tilde{\mathbf{u}}_{kl}^\varepsilon) \cdot \nabla_\mu \hat{\tilde{\mathbf{u}}}_\mu \, \mathrm{d}\Omega_\mu = \underbrace{\int_{\Omega_\mu} \mathbf{P}_\mu(\mathbf{F}_\mu) \cdot \nabla_\mu \hat{\tilde{\mathbf{u}}}_\mu \mathrm{d}\Omega_\mu}_{:=0 \text{ from } (22)} +$$

$$\varepsilon \int_{\Omega_\mu} \mathbb{D}_\mu(\mathbf{F}_\mu)(\mathbf{e}_k \otimes \mathbf{e}_l + \varepsilon^{-1} \nabla_\mu \Delta \tilde{\mathbf{u}}_{kl}^\varepsilon) \cdot \nabla_\mu \hat{\tilde{\mathbf{u}}}_\mu \, \mathrm{d}\Omega_\mu + \mathcal{O}(\varepsilon^2) = 0 \qquad \forall \hat{\tilde{\mathbf{u}}}_\mu \in \mathrm{Var}_{\tilde{\mathbf{u}}_\mu}$$

Since we are interested in the limit when $\varepsilon \to 0$, let $\Delta \tilde{\mathbf{u}}_{kl}$ be:

$$\Delta \tilde{\mathbf{u}}_{kl} = \lim_{\varepsilon \to 0} \frac{1}{\varepsilon} \Delta \tilde{\mathbf{u}}_{kl}^\varepsilon = \lim_{\varepsilon \to 0} \frac{1}{\varepsilon} (\tilde{\mathbf{u}}_\mu^{kl,\varepsilon} - \tilde{\mathbf{u}}_\mu) = \frac{\partial \tilde{\mathbf{u}}_\mu(\mathbf{F} + \varepsilon \mathbf{e}_k \otimes \mathbf{e}_l)}{\partial \varepsilon} \tag{62}$$

So we get the following canonical problem to find $\Delta \tilde{\mathbf{u}}_{kl} \in \mathrm{Var}_{\tilde{\mathbf{u}}_\mu}$:

$$\int_{\Omega_\mu} \mathbb{D}_\mu(\mathbf{F}_\mu) \nabla_\mu \Delta \tilde{\mathbf{u}}_{kl} \cdot \nabla_\mu \hat{\tilde{\mathbf{u}}}_\mu \, \mathrm{d}\Omega_\mu = -\int_{\Omega_\mu} \mathbb{D}_\mu(\mathbf{F}_\mu)(\mathbf{e}_k \otimes \mathbf{e}_l) \cdot \nabla_\mu \hat{\tilde{\mathbf{u}}}_\mu \, \mathrm{d}\Omega_\mu \qquad \forall \hat{\tilde{\mathbf{u}}}_\mu \in \mathrm{Var}_{\tilde{\mathbf{u}}_\mu} \tag{63}$$

Developing (59) in Taylor expansion for the perturbation in kl we have:

$$\lim_{\varepsilon \to 0} \frac{1}{\varepsilon} \left[\mathbf{P}(\mathbf{F} + \varepsilon \mathbf{e}_k \otimes \mathbf{e}_l) - \mathbf{P}(\mathbf{F})\right] \otimes \mathbf{e}_k \otimes \mathbf{e}_l =$$

$$\left[\frac{1}{|\Omega_\mu|} \int_{\Omega_\mu} \lim_{\varepsilon \to 0} \frac{1}{\varepsilon} \left(\mathbf{P}_\mu(\mathbf{F}_\mu + \varepsilon \mathbf{e}_k \otimes \mathbf{e}_l + \nabla_\mu \Delta \tilde{\mathbf{u}}_{kl}^\varepsilon) - \mathbf{P}_\mu(\mathbf{F}_\mu)\right) \, \mathrm{d}\Omega_\mu\right] \otimes \mathbf{e}_k \otimes \mathbf{e}_l =$$

$$\left[\frac{1}{|\Omega_\mu|} \int_{\Omega_\mu} \lim_{\varepsilon \to 0} \mathbb{D}_\mu(\mathbf{F}_\mu)(\mathbf{e}_k \otimes \mathbf{e}_l + \varepsilon^{-1} \nabla_\mu \Delta \tilde{\mathbf{u}}_{kl}^\varepsilon) + \mathcal{O}(\varepsilon) \, \mathrm{d}\Omega_\mu\right] \otimes \mathbf{e}_k \otimes \mathbf{e}_l =$$

$$\frac{1}{|\Omega_\mu|} \int_{\Omega_\mu} (\mathbb{D}_\mu(\mathbf{F}_\mu))_{ijpq}(\mathbf{e}_k \otimes \mathbf{e}_l + \nabla_\mu \Delta \tilde{\mathbf{u}}_{kl})_{pq} \, \mathrm{d}\Omega_\mu \, \mathbf{e}_i \otimes \mathbf{e}_j \otimes \mathbf{e}_k \otimes \mathbf{e}_l =$$

$$\left[\underbrace{\frac{1}{|\Omega_\mu|} \int_{\Omega_\mu} \mathbb{D}_\mu(\mathbf{F}_\mu)_{ijkl} \, \mathrm{d}\Omega_\mu}_{:=\overline{\mathbb{D}}_{ijkl}} + \underbrace{\frac{1}{|\Omega_\mu|} \int_{\Omega_\mu} \mathbb{D}_\mu(\mathbf{F}_\mu)_{ijpq}(\nabla_\mu \Delta \tilde{\mathbf{u}}_{kl})_{pq} \, \mathrm{d}\Omega_\mu}_{:=\widetilde{\mathbb{D}}_{ijkl}}\right] \mathbf{e}_i \otimes \mathbf{e}_j \otimes \mathbf{e}_k \otimes \mathbf{e}_l$$

So we have the following decomposition $\mathbb{D} = \overline{\mathbb{D}} + \widetilde{\mathbb{D}}$ into Taylor and fluctuation contributions.